

Inhibition of C-steel Corrosion in Hydrochloric Solution with *Chenopodium Ambrorsioides* Extract

M. Belkhaouda¹, L. Bammou¹, A. Zarrouk², R. Salghi^{1,*}, E. E. Ebenso³, H. Zarrok⁴, B. Hammouti², L. Bazzi⁵, I. Warad⁶

¹ Equipe de Génie de l'Environnement et de Biotechnologie, ENSA, Université Ibn Zohr, BP 1136, Agadir, Morocco

² LCAE-URAC18, Faculté des Sciences, Université Mohammed Premier, BP 4808, Oujda, Morocco.

³ Material Science Innovation & Modelling (MaSIM) Focus Area, Faculty of Agriculture, Science and Technology, North-West University (Mafikeng Campus), Private Bag X2046, Mmabatho 2735, South Africa

⁴ Laboratoire des procédés de séparation, Faculté des Sciences, Université Ibn Tofail, Kénitra, Morocco.

⁵ LME, Equipe de Physico-Chimie des Matériaux et Environnement, Faculté des Sciences, B.P. 8106, Agadir, Morocco

⁶ Department of Chemistry, Science College, AN-Najah National University, P.O. Box 7, Nablus 00972, Palestine

*E-mail: r_salghi@yahoo.fr

Received: 7 March 2013 / Accepted: 11 April 2013 / Published: 1 May 2013

The behaviour of C-steel in molar hydrochloric acid solution in the presence of *Chenopodium Ambrorsioides* Extract (CAE) was investigated using weight loss measurements, potentiodynamic polarization curves and electrochemical impedance spectroscopy. The results obtained reveal that the aggressiveness of hydrochloric solution was considerably decreased in the presence of the CAE. The inhibition efficiency was found to increase with increase in the concentration of the natural substances tested. Potentiodynamic polarization studies clearly reveal that the presence of CAE does not change the mechanism of the hydrogen evolution reaction and they act essentially as cathodic inhibitors. The temperature effect on the corrosion behaviour of C-steel is studied in the range from 298 to 328K without and with at 0.1 g/l. The adsorption isotherm of natural product on the steel has been determined. The apparent activation energies, enthalpies and entropies of the dissolution process were discussed.

Keywords: inhibition, corrosion, *Chenopodium ambrorsioides* extract, steel

1. INTRODUCTION

Iron and its alloys are frequently used in many industrial applications in various environments because of their excellent combination of properties. Concentrated mineral acids used extensively in pickling, cleaning, desiccating and well activities caused corrosion damage to many metals and alloys [1-4]. From the economic point of view, the inhibition of corrosion of these metals in different aqueous solutions is very important. Many methods reduce the rate of metallic corrosion. Among these, addition of inhibitors is a practical technique to secure metals and alloys from aggressive environments. Several works have studied the influence of organic compounds containing nitrogen, oxygen, sulphur atoms on the corrosion of steel in acidic media [5-17]. These studies have been reported to exhibit good inhibiting properties.

Recently, several researchers have focused their works on the use of natural products named green inhibitors, as corrosion inhibitors [18-29]. Among these compounds tested in our laboratory, we cite extract compounds such as; Verbena extract [30], Chamomile extract [31], *Marrubium Vulgare L.* extract [32], Argan extracts [33-36] and oil compounds such as: Chamomile essential oil [37], Carob seed oil [38], Verbena essential oil [39], Prickly pear seed oil [40], Argan oil [41, 42], Fennel oil [43], *Thymus oil* [44]. These compounds tested have been reported to be excellent inhibitors for metals and alloys in acidic solutions.

The aim of the present work is to study the effect of the *Chenopodium Ambrorsioides* extract on the behaviour of steel corrosion in molar hydrochloric solution.

2. EXPERIMENTAL

C steel specimens used for the study have the composition given in Table 1

Table 1. Chemical composition of C-steel

Element	C	Si	Mn	Cu	S	Fe
Weight%	0.179	0.165	0.439	0.203	0.034	balance

The aggressive solution of 1M HCl was prepared by dilution of Analytical Grade 37% HCl with double distilled water. All experiments were carried out in molar hydrochloric acid solution in the absence and presence of different concentrations (10^{-4} , 10^{-3} , $5 \cdot 10^{-2}$, 10^{-2} and 10^{-1} g/l) of *Chenopodium Ambrorsioides* Extract. The cross section of the working electrode (0.32 cm² area) was mechanically ground with emery paper up to 1200 grade, degreased in acetone and rinsed with bidistilled water before immersed in the test solution.

Polarisation measurements and EIS measurements were carried out in a conventional three-electrode electrolytic cell. Saturated calomel electrode (SCE) and platinum electrode were used as reference and auxiliary electrodes respectively.

Gravimetric measurements were carried out in a double walled glass cell equipped with a thermostat cooling condenser. The C-steel specimens of size 2 cm×1cm×0.3cm in 1M of hydrochloric acid containing different concentrations (10^{-4} , 10^{-3} , 5.10^{-2} , 10^{-2} and 10^{-1} g/l) of CAE at 298K for 06 h. The solution volume was 100 ml.

A Potentiodynamic polarization measurement was carried out using Voltalab PGZ 100 piloted by ordinate associated to "Volta Master 4" software. The scan rate was 0.5 mV/s started from an initial potential of -800 to -100 mV/SCE. Before recording each curve, the working electrode is maintained with its free potential of corrosion during 30 minutes. All experiments were repeated three times at temperature desired $\pm 1^\circ\text{C}$. Corrosion current densities were obtained from the polarization curves by linear extrapolation of the Tafel curves.

Electrochemical impedance spectroscopy (EIS) was carried out with a same equipment was used as for the Tafel polarization measurements, leaving the frequency response analyser out of consideration. Quasi-potentiostatic polarization curves were obtained using a sweep rate of 1 mVs^{-1} . After the determination of steady-state current at a given potential, sine wave voltage (10 mV) peak to peak, at frequencies between 100 kHz and 10 mHz were superimposed on the rest potential. Computer programs automatically controlled the measurements performed at rest potential after 30 min of exposure. All potentials were reported versus saturated calomel electrode (SCE). The impedance diagrams are given in the Nyquist representation. Experiments are repeated three times to ensure the reproducibility

3. RESULTS AND DISCUSSION

3.1. Weight loss tests

The C-steel were abraded with a series of emery paper (grade 800-1200) and then washed thoroughly with acetone and distilled water. After weighing precisely, the specimens were immersed in beakers which contained 100 ml acid solutions with different concentrations of CAE at a certain temperature remained by a water thermostat.

All the aggressive acid solutions were open to air. After 06 h the specimens were taken out, washed, dried, and weighed accurately. In order to get good reproducibility. The inhibition efficiencies $E_w(\%)$ corrosion was calculated from the following equation:

$$E_w(\%) = \left(1 - \frac{W_{cor}}{W_{cor}^0}\right) \cdot 100 \quad (1)$$

where W_{cor}^0 and W_{cor} are the corrosion rates of C-steel due to the dissolution in 1 M HCl in the absence and the presence of definite concentrations of the inhibitor, respectively.

Table 2 gives the inhibition efficiencies (E_w) and the gravimetric corrosion rates (W_{cor}) of C-steel for different concentrations of CAE in molar hydrochloric acid solutions at 298K.

Table 2. C-steel weight loss data and inhibition efficiency of *Chenopodium Ambrorsioides* Extract.

Conc. (g/l)	W_{cor} (mg. cm ⁻² .h ⁻¹)	E_w (%)
Blank	1.84	--
10 ⁻⁴	0.9	51
10 ⁻³	0.52	72
5.10 ⁻²	0.35	81
10 ⁻²	0.26	86
10 ⁻¹	0.16	91

Results obtained from gravimetric measurements show for inhibitor tested that the corrosion rate values decrease when the concentration of CAE increases. Inhibition efficiency increases with increasing of inhibitor concentration and reaches a maximum at 10⁻¹ g/l.

3.2. Polarization results

The potentiodynamic polarization curves of the C-steel electrode in molar hydrochloric acid in absence and presence of various concentrations of CAE plotted at 298K are shown in Fig.1. Electrochemical parameters obtained from the polarization curves are shown in Table 3. These incorporate corrosion potential (E_{cor}), corrosion current density (I_{cor}) determined by extrapolation of the cathodic Tafel line to the corrosion potential, cathodic Tafel slope (b_c). The inhibition efficiency E_p (%) is calculated by the relation:

$$E_p (\%) = \left(1 - \frac{I_{cor}}{I_{cor}^0}\right) \cdot 100 \quad (2)$$

where I_{cor} and I_{cor}^0 were the corrosion current densities without and with inhibitor.

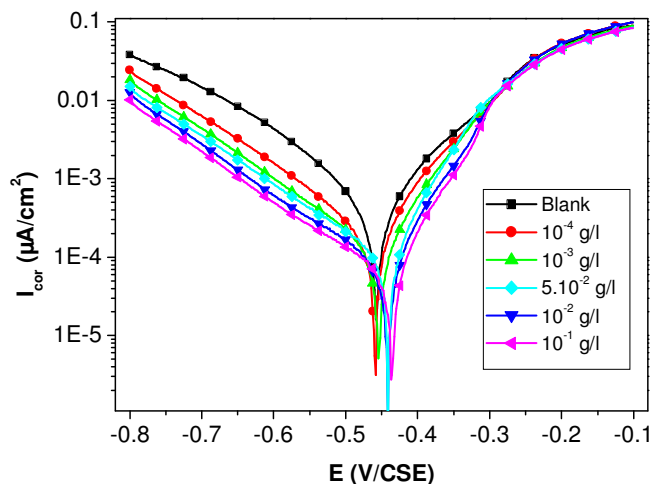
**Figure 1.** Polarization curves for C-steel in 1M HCl at various concentrations of CAE at 298K

Table 3. Electrochemical parameters for C-steel in 1M HCl at various concentrations of CAE at 298K

Conc. (g/l)		E_{cor} (mV/SCE)	bc (mV/dec)	E_p (%)
blank	594	-457	-204	--
10^{-4}	259	-462	-173	56.39
10^{-3}	180	-454	-160	69.69
$5 \cdot 10^{-2}$	96	-442	-166	83.83
10^{-2}	76	-444	-157	87.20
10^{-1}	58	-436	-155	90.23

The result obtained from polarisation curves show that the addition of the Chenopodium ambrorsioides at different concentrations decreases in the cathodic current densities. This behaviour reflects its capacity to inhibit the corrosion of C-steel in HCl solution. Tafel behaviour characterised by linear regions in the vicinity of the corrosion potential indicates that the hydrogen evolution reaction is activation controlled. The addition of the Chenopodium ambrorsioides to the corrosive solution modifies the cathodic Tafel slope (bc) and then the mechanism of the process is affected. The free corrosion potential determined after 30 min of immersion does not change in the presence of the inhibitor. These results demonstrated that the hydrogen evolution reaction is inhibited and that the inhibition efficiency increases with inhibitor concentration. The inhibiting action is increased with the concentration to reach the maximum value of 90.23% at the 10^{-1} g/l.

3.3. Electrochemical impedance spectroscopy measurements

The corrosion behaviour of c-steel in 1M HCl solution in the absence and presence at various concentrations of Chenopodium ambrorsioides inhibitor is investigated by the electrochemical impedance spectroscopy (EIS) at 298 K after 30 min of immersion. Fig.2. shows the EIS diagrams plotted at open circuit potential (E_{corr}) and obtained as Nyquist plots. The parameters associated with the impedance diagrams such as charge transfer resistance (R_t), double-layer capacitance (C_{dl}), and frequency (f_{max}) determined from Nyquist plots and inhibition efficiency (E_{EIS}) got from the charge-transfer resistance summarised in Table 4. The inhibition efficiency calculated from the charge transfer resistance by the following relation:

$$E_{EIS}(\%) = \left(1 - \frac{R_t}{R_t^0}\right) \cdot 100 \quad (3)$$

Where R_t and R_t^0 are the transfer resistance in the absence and presence of Chenopodium ambrorsioides inhibitor, respectively. The charge transfer resistance value is the diameter of the loop. The impedance curves obtained present one single capacitive loop. This capacitive loop indicates that the corrosion of steel is mainly controlled by the charge transfer process [45]. The diameter of the capacitive loop increased after the addition of inhibitors to the corrosive solution. This behaviour show

that the impedance of inhibited substrate increases with the inhibitor concentration, and lead to excellent inhibitive performance.

The value of double-layer capacitance (C_{dl}) evaluate by equation:

$$C_{dl} = \frac{1}{2 \pi \cdot R_t \cdot f_{max}} \quad (4)$$

decreases on the addition of inhibitors, this decrease is attributed to a decrease in the local dielectric constant and/or an increase in the thickness of the formed layer by adsorption of inhibitor at the metal surface[46]. These suggestions based to the following relation [47]:

$$C_{dl} = \frac{\epsilon \epsilon_0 S}{\delta} \quad (5)$$

Where δ is the thickness of the protective layer, S is the surface of the used electrode, ϵ_0 is the permittivity of the air and ϵ is the dielectric constant of medium. The value of R_t and E_{EIS} (%) increases with increasing extract concentration. This behaviour can be attributed to the formation of protective film on the metal/solution interface.

The inhibition efficiency value calculated from EIS data is in good agreement with those obtained from electrochemical polarization and weight loss methods.

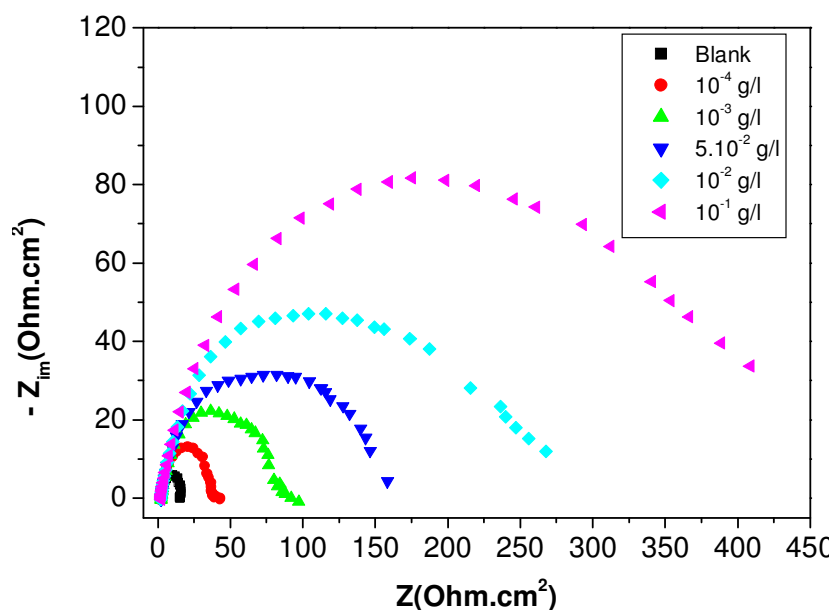


Figure 2. Nyquist plots of C-steel in 1 M HCl without and with different concentrations of CAE at 298K

The value of C_{dl} decrease with increasing of the inhibition efficiency. This behaviour is due to the adsorption of the inhibitor on the electrode surface leading to the formation of film or complex from acidic solution [48].

Table 4. Impedance parameters for corrosion of steel in 1M HCl without and with different concentrations of CAE at 298 K.

Conc. (g/l)				
Blank	15.0	92	116	--
10 ⁻⁴	36.6	48	90	58.33
10 ⁻³	65.0	29	83	76.92
5.10 ⁻²	148.0	25	43	89.86
10 ⁻²	170.0	20	47	91.17
10 ⁻¹	350.0	14	32	95.71

3.4. Effect of temperature

The effect of temperature on the corrosion behaviour of C steel studied using polarization methods at the temperature in the range 298 – 328K in the absence (Fig. 3) and the presence of inhibitor at 0.1 g/l (Fig. 4) in 1M HCl. Table 5 summered the electrochemical parameters deduced from the polarization curves and inhibition efficiency determined by relation (2)

From these results, we note the important elevation of corrosion rate when the temperatures of blank solution increase. In the presence of the tested inhibitor, the dissolution of C steel is extensively retarded. The inhibitive efficiency of the inhibitor tested is not affected with the rise of temperature.

The plot of $\log(I_{cor})$ and $\log(I_{cor}/T)$ for C steel in 1M HCl in absence (Fig. 5) and presence of CAE at 0.1g/l (Fig. 6), respectively, can be represented as a straight-line function of $10^3/T$, where T is the temperature in Kelvin.

The activation parameters such as the activation energy E_a , the activation enthalpy ΔH_a^* and the activation entropy ΔS_a^* for the corrosion of C-steel in 1M HCl were estimated using Arrhenius equation and transition state equation

$$I_{cor} = A \exp\left(-\frac{E_a}{RT}\right) \quad (6)$$

$$I_{cor} = \frac{RT}{Nh} \exp\left(\frac{\Delta S_a^*}{R}\right) \exp\left(-\frac{\Delta H_a^*}{RT}\right) \quad (7)$$

where A is the Arrhenius pre-exponential factor, R is the perfect gas constant, N is the Avogadro's number and h is the Plank's constant. The values of E_a , ΔH_a^* and ΔS_a^* were estimated from the precedent equations given in Table 6.

The positive sign of ΔH_a^* show that the corrosion process of c steel is an endothermic phenomenon signifying that its dissolution is slow in the presence of CAE [49]. The positive sign of ΔS_a^* indicate that an increase in disordering occurs in going from reactants to the electrode/solution interface which is the driving force for the adsorption of inhibitor on the steel surface [50,51].

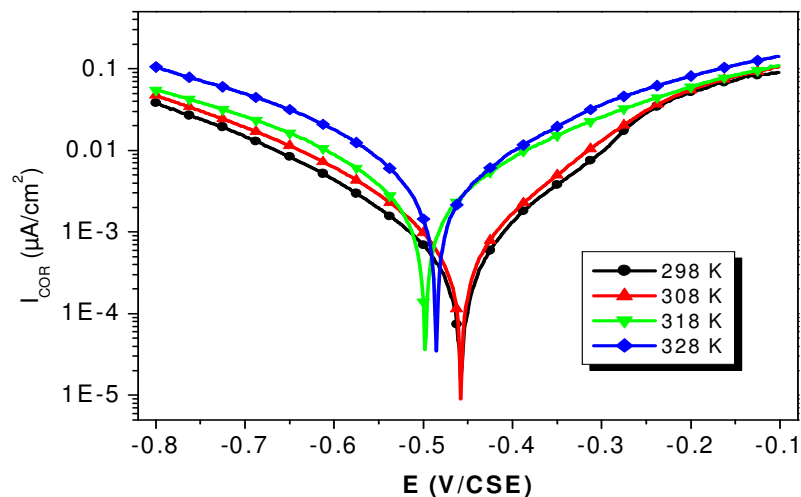


Figure 3. Polarisation curves for C-steel in 1M HCl at different temperature

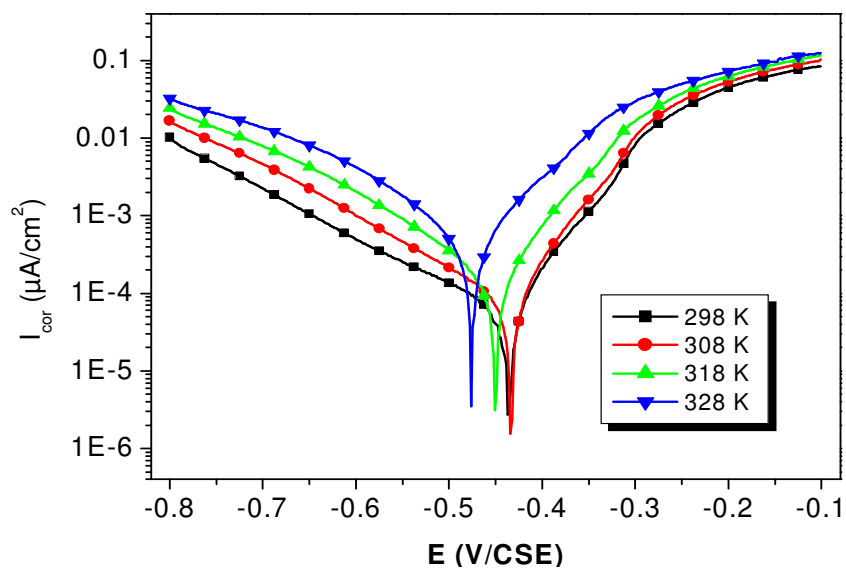


Figure 4. Polarisation curves for C-steel in 1M HCl + 0.1g/l CAE at different temperature

Table 5. Electrochemical parameters for corrosion of steel in 1M HCl at different temperatures in the absence and presence of 0.1 g/L CAE

Concentration	T (K)	E _{cor} (mV/SCE)	I _{cor} (μA/cm ²)	bc (mV/dec)	E _p (%)
Blank	298	-457	594	-204	--
	308	-458	900	-199	--
	318	-500	3360	-214	--
	328	-487	6820	-234	--
0.1 g/l	298	-436	58	-155	90.23
	308	-433	82	-147	90.88
	318	-450	247	-166	92.64
	328	-474	460	-188	93.25

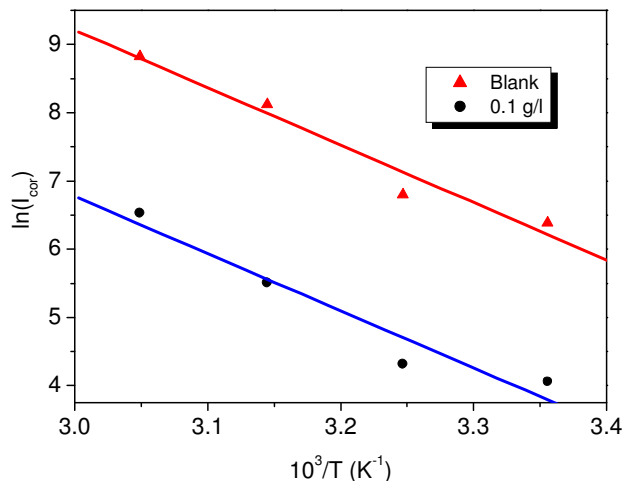


Figure 5. Arrhenius plots of C-steel in 1 M HCl with and without 0.1 g/L CAE.

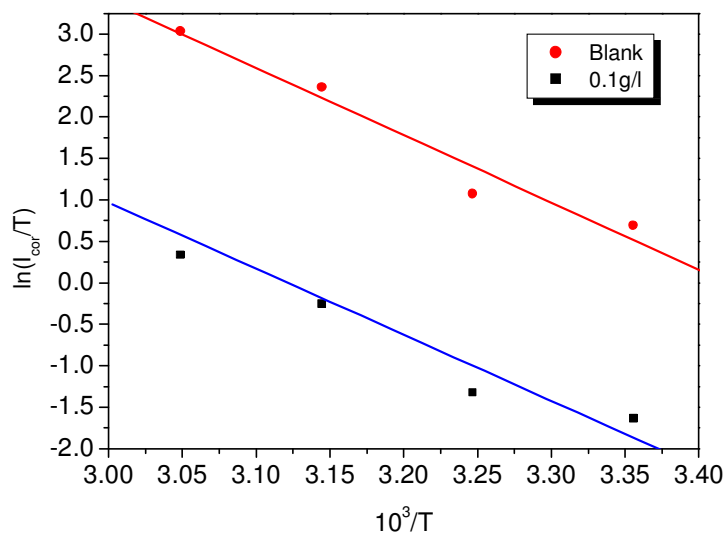


Figure 6. Variation of Ln (I_{corr}/T) versus 10³/T for blank and 1M HCl + 0.1 g/l of CAE.

Table 6. The value of activation parameters for steel in 1M HCl in the absence and presence of 0.1 g/l of CAE.

	E_a (kJ.mol ⁻¹)	ΔH_a^* (kJ.mol ⁻¹)	ΔS_a^* (J.mol ⁻¹ .K ⁻¹)
Blank	70.01	67.43	32.95
0.1g/l	59.23	56.63	- 16.03

3.6. Adsorption isotherm

Adsorption isotherms are very important in determining the behaviour of the inhibitor on the electrode surface. The surface coverage values (θ) were evaluated using inhibitive efficiency values

obtained from the polarization methods. The increase in inhibition efficiencies with increasing concentration extract can be caused by adsorption of inhibitor on the C-steel surface and conforms to the Langmuir adsorption isothermal equation:

$$\frac{C_{inh}}{\theta} = \frac{1}{k_{ads}} + C_{inh} \quad (8)$$

where C_{inh} is the Concentration of CAE and k_{ads} is the adsorption equilibrium constant of the adsorption process.

A straight line was obtained by plotting the graph of C_{inh} vs C_{inh}/θ with the R value almost unity (0.9999) (Fig. 7). The slope is reported almost unity suggesting that the Langmuir adsorption isotherm model provides the best description of the adsorption behaviour.

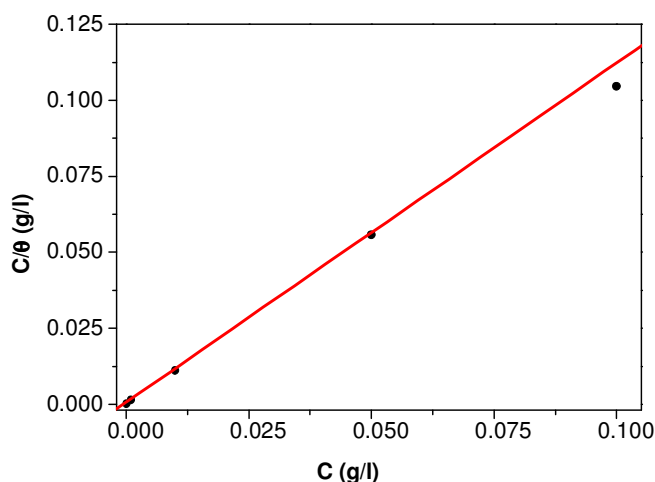


Figure 7. Langmuir isotherm adsorption of CAE on the C-steel electrode in 1M HCl. (EIS)

4. CONCLUSION

The principal result of the present work can be recapitulated as follows:

- CAE mainly acts as excellent inhibitor for the corrosion of steel in 1 M HCl.
- Inhibition efficiency increases with the inhibitor concentration.
- The inhibition efficiency increases with temperature.
- The inhibition efficiency determined by gravimetric, EIS and polarization methods are in good agreement.
- The adsorption of CAE on the steel surface obeys to the Langmuir isotherm model.

References

1. I. Ahamad, R. Prasad, M.A. Quraishi, *Corros. Sci.* 52 (2010) 1472.

2. A. K. Singh, M.A. Quraishi, *Corros. Sci.* 52 (2010) 152.
3. L.R. Chauhan, G. Gunasekaran, *Corros. Sci.* 49 (2007) 1143.
4. Y. Abboud, A. Abourriche, T. Saffaj, M. Berrada, M. Charrouf, A. Bannamara, N. Al-Himidi, H. Hannache, *Mater. Chem. Phys.* 105 (2007) 1.
5. S.D. Ben Hmamou, R. Salghi, A. Zarrouk, H. Zarrok, B. Hammouti, S. S. Al-Deyab, M. Bouachrine, A. Chakir, M. Zougagh. *Int. J. Electrochem. Sci.*, 7 (2012) 5716.
6. D. Ben Hmamou, R. Salghi, A. Zarrouk, B. Hammouti, O. Benali, H. Zarrok S. S. Al-Deyab. *Res Chem Intermed* DOI 10.1007/s11164-012-0892-3 (2012).
7. D. Ben Hmamou, R. Salghi, A. Zarrouk, H. Zarrok, S. S. Al-Deyab, O. Benali, B. Hammouti. *Int. J. Electrochem. Sci.*, 7 (2012) 8988.
8. M. Bouklah, B. Hammouti, M. Lagrenée, F. Bentiss, *Corros. Sci.* 48 (2006) 2831.
9. L. Herrag, B. Hammouti, S. Elkadiri, A. Aouniti, C. Jama, H. Vezin, F. Bentiss, *Corros. Sci.* 52 (2010) 3042.
10. B. Hammouti, A. Dafali, R. Touzani, M. Bouachrine. *Journal of Saudi Chemical Society* 16 (2012) 413
11. S. E. Nataraja, T. V. Venkatesha, K. Manjunatha, B. Poojary, M. K. Pavithra, H.C. Tandon, *Corros. Sci.* 53 (2011) 2651.
12. F. Bentiss, C. Jama, B. Mernari, H. El Attari, L. El Kadi, M. Lebrini, M. Traisnel, M. Lagrenée. *Corros. Sci.* 51 (2009) 1628.
13. N. Soltani, M. Behpour, S.M. Ghoreishi, H. Naeimi. *Corros. Sci.* 52 (2010) 1351.
14. P. Lowmunkhong, D. Ungthararak, P. Sutthivaiyakit. *Corros. Sci.* 52 (2010) 30.
15. G. Quartarone, L. Ronchin, A. Vavasori, C. Tortato, L. Bonaldo. *Corros. Sci.* 64 (2012) 82.
16. H. Zarrok, A. Zarrouk, B. Hammouti, R. Salghi, C. Jama, F. Bentiss. *Corros. Sci.* 64 (2012) 243.
17. L. Li, Q. Qu, W. Bai, F. Yang, Y. Chen, S. Zhang, Z. Ding. *Corros. Sci.* 59 (2012) 249.
18. M. Znini, L. Majidi, A. Bouyanzer, J. Paolini, J.-M. Desjobert, J. Costa, B. Hammouti. *Arabian Journal of Chemistry*. 5 (2012) 467.
19. M. Dahmani, S.S. Al-Deyab, A. Et-Touhami, B. Hammouti, A. Bouyanzer, R. Salghi, A. El Mejdoubi, *Int. J. Electrochem. Sci.* 7 (2012) 2513.
20. N. Lahhit, A. Bouyanzer, J.M. Desjobert, B. Hammouti, R. Salghi, J. Costa, C. Jama, F. Bentiss, L. Majidi, *Port. Electrochim Acta.* 29 (2011) 127.
21. S. Deng, X. Li, *Corros. Sci.* 55 (2012) 407.
22. N. Soltani, N. Tavakkoli, M. Khayatkashani, M. R. Jalali, A. Mosavizade, *Corros. Sci.* 62 (2012) 122.
23. Xianghong Li, Shuduan Deng, Hui Fu, *Corros. Sci.* 62 (2012) 163.
24. K.O. Orubite, N.C. Oforka, *Materials Letters.* 58 (2004) 1768.
25. A. Lecante, F. Robert, P.A. Blandinières, C. Roos. *Current Applied Physics* . 11 (2011) 714.
26. M. Lebrini, F. Robert, A. Lecante, C. Roos, *Corros. Sci.* 53 (2011) 687.
27. O. Benali, C. Selles, R. Salghi. *Res Chem Intermed.* DOI 10.1007/s11164-012-0960-8 (2012).
28. L. Bammou, M. Mihit, R. Salghi, L. Bazzi, A. Bouyanzer, B. Hammouti, *Int. J. Electrochem. Sci.* 6(2011) 1454
29. M. Larif, A. Elmidaoui, A. Zarrouk, H. Zarrok, R. Salghi, B. Hammouti, H. Oudda, F. Bentiss. *Res Chem Intermed.* DOI 10.1007/s11164-012-0788-2. (2012).
30. D. Ben Hmamou, R. Salghi, A. Zarrouk, S. S. Al-Deyab, H. Zarrok, B. Hammouti, E. Errami. *Int. J. Electrochem. Sci.* 7 (2012) 6234.
31. D. Ben Hmamou, R. Salghi, A. Zarrouk, M. Messali, H. Zarrok, M. Errami, B. Hammouti, Lh. Bazzi, A. Chakir. *Der Pharma Chemica*, 4(4) (2012) 1496.
32. D. Ben Hmamou, R. Salghi, A. Zarrouk, H. Zarrok, O. Benali, M. Errami, B. Hammouti. *Res Chem Intermed* DOI 10.1007/s11164-012-0840-2
33. D. Ben Hmamou, R. Salghi, L. Bazzi, B. Hammouti, S.S. Al-Deyab, L. Bammou, L. Bazzi, A. Bouyanzer, *Int J Electrochem. Sci.*, 7 (2012) 1303.

34. L. Afia, R. Salghi, L. Bazzi, M. Errami, O. Jbara, S.S. Al-Deyab, B. Hammouti, *Int J Electrochem. Sci.* 6 (2011) 5918.
35. L. Afia, R. Salghi, L. Bammou, E. Bazzi, B. Hammouti, L. Bazzi, *Acta Metall. Sin.* 25 (2012) 10.
36. L. Afia, R. Salghi, E. Bazzi, A. Zarrouk, B. Hammouti, M. Bouri, H. Zarrouk, L. Bazzi, L. Bammou. *Res Chem Intermed.* doi:10.1007/s11164-012-0496-y (2012).
37. D. Ben Hmamou, R. Salghi, A. Zarrouk, B. Hammouti, S.S. Al-Deyab, Lh. Bazzi, H. Zarrok, A. Chakir, L. Bammou. *Int. J. Electrochem. Sci.* 7 (2012) 2361.
38. D. Ben Hmamou, R. Salghi, A. Zarrouk, O. Benali, F. Fadel, H. Zarrok, and B. Hammouti. *International Journal of Industrial Chemistry* . 3 (2012) 25.
39. D. Ben Hmamou, R. Salghi, A. Zarrouk, H. Zarrouk, M. Errami, B. Hammouti, L. Afia, Lh. Bazzi, L. Bazzi. *Res Chem Intermed.* DOI 10.1007/s11164-012-0609-7.
40. D. Ben Hmamou, R. Salghi, A. Zarrouk, B. Hammouti, S. S. Al-Deyab, Lh. Bazzi, H. Zarrok, A. Chakir, L. Bammou, *Int. J. Electrochem. Sci.* 7 (2012) 2361.
41. L. Afia, R. Salghi, L. Bammou, El. Bazzi, B. Hammouti, L. Bazzi, A. Bouyanzer, *J. Saudia Chemistry Science* (2011) doi.org/10.1016/j.jscs.2011.05.008.
42. L. Afia, R. Salghi, El. Bazzi, L. Bazzi, M. Errami, O. Jbara, S. S. Al-Deyab, B. Hammouti, *Int. J. Electrochem. Sci.* 6 (2011) 5918.
43. N. Lahhit, A. Bouyanzer, J. M. Desjobert, B. Hammouti, R. Salghi, J. Costa, C. Jama, F. Bentiss and L. Majidi, *Port. Electrochim. Acta.* 29 (2011) 127.
44. L. Bammou, B. Chebli, R. Salghi, L. Bazzi, B. Hammouti, M. Mihit and H. El Idrissi, *Green. Chem. Lett. Rev.* 3 (2010) 173.
45. M. Hukovic-Metikos, R. Babik, Z. Grotac, *J. Appl. Electrochem.* 32 (2002) 35.
46. E. McCafferty, N. Hackerman, *J. Electrochem. Soc.* 119 (1972) 146.
47. E.E. Oguzie, Y. Li, F.H. Wang, *Electrochim. Acta.* 53 (2007) 909.
48. F. Bentiss, M. Lagrenée, M. Traisnel, J.C. Hornez, *Corros. Sci.* 41(1999)789.
49. N.M. Guan, L. Xueming, L. Fei, *Mater. Chem. Phys.* 86 (2004) 59.
50. G. Banerjee, S.N. Malhotra, *Corrosion.* 48 (1992) 10.
51. X.H. Li, S.D. Deng, H. Fu, G.N. Mu, *Corros. Sci.* 50 (2008) 2635.